

**Military Technical College
Kobry El-Kobbah,
Cairo, Egypt.**



**15th International Conference
on Applied Mechanics and
Mechanical Engineering.**

ON THE SENSITIVITY OF CUTTING CONDITIONS ON CUTTING FORCES AND VIBRATION SIGNALS WHEN TURNING WITH TOOL INSERTS WITH INTEGRATED CHIP-BREAKER GEOMETRY

E. Dimla*

ABSTRACT

This paper is concerned with investigating the effects of cutting conditions on sensor signals, employing tool inserts with chip breaker geometry and a harder workpiece material. Medium double coated carbide grade tool inserts with integral groove chip-breaker was used to cut EN24T alloy steel. The focus was to investigate and corroborate the effects of cutting conditions (cutting speed, feed rate and dept of cut) on the cutting forces and vibrations signals during orthogonal turning using coated chip-breaker geometry indexable tool inserts. Cutting forces and vibration signals were recorded on-line at the various cutting conditions, and these analysed in time and frequency modes for features that were sensitive to the variation in the cutting conditions. Peculiar characteristics in the signal spectrum were identified and these were easily associated with changes in the cutting conditions as well as chip lamination.

KEY WORDS

Metal turning, chip breaker inserts, cutting forces, vibration signature, tool wear, cutting conditions.

* Lecturer, School of Engineering, University of Portsmouth, Portsmouth, U. K. Email: Eric.Dimla@port.ac.uk

INTRODUCTION

Research in metal cutting has been performed for well over a century now, but researchers are not significantly closer to quantitatively predicting many aspects of the cutting process. For example, it is not yet possible to predict, with any great accuracy, the forces involved in orthogonal metal cutting due to the complexity of the mechanics of the cutting process and the characteristic lack of geometrical constraint due to linkages and bearings. Figure 1 shows the most commonly used terms and tool geometry definition of a typical metal cutting tooling system.

A metal cutting operation can generally be viewed as consisting of a number of semi-independent systems. A complex and dynamically varying system forms between the workpiece and the cutting tool, with the cutting forces, power requirements, vibrations, temperature, acoustic emission, etc. having a non-linear relationship with wear accrual on the cutting tool edges. The cutting tool variables can be measured through the application of sensors, and their behaviour monitored to effect in predicting tool wear. The sole aim of such investigations has been to establish distinctive sensor signal characteristics whose trend could be monitored to determine cutting tool wear.

Two kinds of metal cutting operations in turning can usually be encountered; oblique and orthogonal cutting. Orthogonal cutting, could be argued, represents a reasonable approximation of cutting on the major cutting edges and, therefore is the most prevalent form of cutting [1]. In orthogonal cutting, the cutting tool approaches the workpiece at right angles to the direction of cutting, with the cutting edge parallel to the uncut surface.

Cutting parameters (depth of cut, feed rate and cutting speed) are chosen so as to be consistent with the strength of the part, chunk, power of machine and amount of stock to be removed. As depth of cut increases, the cutting force becomes larger, and must therefore be limited to the available power of the machine. Feed rate depends on the finish desired, strength of machine and its rigidity. Finishing cuts require a light feed rate whereas roughing cuts are often large with the cutting speeds dependent entirely on workpiece hardness. Several other machining processes can be performed in conjunction with turning, such as facing, reaming, boring, etc. although less frequently. The only restriction in turning seems to be the availability of equipment size, to hold and rotate the workpiece, with problems in holding and handling as size and weight increases. A full understanding of the mechanics of the orthogonal cutting process is not intended to be discussed in this research as it is out of the scope of the work. It is however fair to assume that high stresses and strain rates develop as the cutting tool ploughs through the workpiece giving rise to complicated forces, high temperatures, and dynamic behaviour across a broad spectrum of frequencies. The cutting force (F) can be resolved into three mutually perpendicular force components: the Tangential Force F_t (F_z), the Feed Force F_f (F_x) and the Radial Force F_r (F_y) as depicted in Fig. 3. These components fluctuate and their excursions give rise to machine chattering (tool holder vibrations manifested on the workpiece by saw-tooth marks and serrations on the underside of chip).

Orthogonal cutting generates considerable amounts of heat and energy at a rate proportional to both the cutting speed and the resultant tool force. Elastically deforming materials generate a small amount of energy and usually this energy is stored in the material as strain energy. Plastically deforming materials generate large amounts of heat, as the material of the workpiece is subjected to high strain levels that are converted to heat energy at the zones of primary and secondary deformation as depicted on Fig.3 [2]. Some heat also arises due to friction between the tool and the new workpiece surface.

Dynamic and static forces constitute the cutting forces in any metal cutting operation. The static force gives an indication of force magnitude levels, whereas the dynamic force represents the degree of fluctuation in the cutting force. Generally, two main classes of chips are produced from metal cutting: continuous and discontinuous, sometimes with built-up edge (BUE) and serration occurring between them [3]. The two categories of chips formed are not so easily defined as both shades of gradation between the two types can be observed. Discontinuous chips are desirable as they are easy to clear from the working area and chip-breakers (Fig. 1(a) and Fig. 1(b)), an integral groove in the rake face or a separate piece fastened to the tool used to cause the chip to break into short sections or curl. Continuous chips could become entangled in the machine tool posing a serious problem to the machine operator.

Continuous chip usually forms at a high cutting speed or high rake angle as the material deformation occurs principally in the primary shear zone. Discontinuous chip results from a combination of material property, low rake angle, very low or very high cutting speed and the secondary shear zone.

Movement of the chip and workpiece across the face of the cutting tool has in the past been inappropriately treated as classical friction situations, but detailed studies have shown this not to be the case [4]. Under certain conditions (low cutting speeds and high feed rates), the flow of chip from the cutting tool is such that it welds itself onto the cutting tool. This increases the friction on the cutting edge, leading to a building-up of more layers of chip material on the tool (Fig. 3) commonly referred to as BUE [2, 4, 5].

This study aims to investigate the effects of cutting conditions on sensor signals, employing double coated tool inserts with integrated chip breaker geometry in the machining of a hard workpiece material, EN24T alloy steel. Details of the cutting conditions, material and tooling inserts are provided in summary Table 1. A schematic of the test bed utilised is shown in Fig. 4.

The experimental design and machining tests conducted in this investigation utilised the same test equipment as described in Dimla [6]. The experimental details (cutting conditions, tool geometry and coating) is presented in Section 2 together with the workpiece material composition and experimental conditions. The processed and correlated results acquired is presented and discussed in Sections 3-5. An appendix is included containing a formal description of the signal processing as well as a description of the theoretical interpretation of the signal processing algorithm.

EXPERIMENTAL DETAILS

Details of the cutting conditions, material and tooling inserts are provided in summary Table 1. The duration of each test cut was such that stabilisation of the cutting process would be attained, and recording of the sensor signals was carried out after 5-10 seconds had elapsed. During each test cut, the active cutting time or time of tool engagement, chip samples as well as features of significance on the tool surface such as wear and built-up edge (BUE) were recorded, in addition to the cutting forces and vibration levels in all three principal directions.

In summary, test cuts were conducted under the following conditions:

Test Set 1: Involved investigating the effects of cutting speed on the sensor signals. The cutting speed (v) was varied from 100 m/min to 300 m/min at 20 m/min intervals at a feed rate (f) of 0.2 mm/rev and depth of cut (a) of 2 mm.

Test Set 2: The feed rate was varied from 0.076 mm/rev to 0.42 mm/rev with five values in between. The cutting speed used was 200 m/min and a constant Depth of cut (DOC) of 2 mm.

Finally, **the 3rd set of tests** involved investigating the effects of DOC variation on the signals. The DOC was varied from 0.5 mm to 3 mm at 0.5 mm intervals with a feed rate and cutting speed of 0.1 mm/rev and 200 m/min respectively.

Medium double-coated carbide grade tool inserts (integral groove chip-breaker geometry) of the P15 (TiN outer coating and Al₂O₃ inner coating) type was used to cut EN24T steel. In line with ISO 3685, flank wear was selected in this study as the basis for tool wear measurement. ISO 3685 states that for a cemented tool insert to be considered sharp, the minimum flank wear on an evenly distributed face should not exceed 0.3 mm, whereas, for uneven or badly grooved, chipped or scratched cutting tool faces, the maximum should not exceed 0.6 mm. All the tests were conducted with the tool in the sharp phase and results were analysed in both the time and frequency domains [7-9], with the objective being to establish the nature and level of sensor signal component change i.e. their sensitivity to process parameter variation.

The sensor signal processing aimed at extracting features that best described the characteristics of the process conditions. Signals from the metal cutting process generally are non-stationary due to the non-linearity of the cutting process and workpiece inhomogeneities. The statistical mean of the sampled cutting force was chosen to describe the nature of the static force behaviour since the signal was assumed to be stationary, and its mean therefore remained constant throughout a cutting pass. With the static force known for each cutting pass, \bar{F} , the dynamic or time varying force, $F_d(i)$, component for each data point could be determined for each i^{th} data point as the difference between the F_i and the \bar{F} .

Further data processing was conducted to reduce the size of the sampled data and alleviate collinearity among the dynamic signal components. Details of the algorithm and theory are presented in the appendix.

TIME DOMAIN ANALYSIS

Effects of Speed Change

Inspection of the static force displays (Fig. 5) showed that the three static force components were affected to a varying degree, by cutting speed changes. The x-component magnitude (418N) initially decreased as the speed was increased from 100 m/min. but then decreased to a minimum value of 407N at $V = 180\text{m/min}$. It then rose to 450N at $V = 300\text{m/min}$. The z-component decreased erratically, with no discernible trend being immediately apparent. The sum total power (STP) dynamic force (Fig. 6) also showed sensitivity to changes in the cutting speed, with the z-axis component being the most sensitive to cutting speed changes.

Increases in the cutting speed lead to a concurrent rise in STP dynamic forces, peaking at 180 m/min. and then decreasing gradually. The STP acceleration signals (Fig. 7) tended to behave similarly to the STP dynamic force signals, but with the x-component being the most sensitive to speed changes.

Effects of Feed Rate

The static force plots (Fig. 8) showed that the z-component was the most sensitive to feed rate changes and the y-component the least. At faster feed rates (i.e. above 0.1 mm/rev), the force components behave in a linear manner with larger changes occurring in the z-axis than the x- and y-axes. Both the STP dynamic force components (Fig. 9) were sensitive to feed rate variation, with the z-component being the most sensitive, increasing nearly 25% in magnitude for a step increment in feed rate. The z- and x-STP acceleration (Fig. 10) behaved identically to the STP dynamic force, while the x-component was not sensitive at all.

Effects of Depth of Cut

As the DOC increased from 0.5 mm to 3 mm both the x- and z-components of the static force showed a linear sensitivity with a constant slope (Fig. 11). The y-component of static force showed only a slight increase. As for the STP dynamic force (Fig. 12), all three components were sensitive (to an extent) to DOC increments with the z-STP dynamic force component having the largest slope and the y-axis the least. The acceleration components (Fig. 13) showed that the x- and z-vibrations were most affected by increases in the DOC.

The sensitivity of the sensor signals to changes in the cutting conditions can be summarised by building a sensitivity index table by assigning numbers (i.e. high when sensitive and low when not). Such a table was constructed using the following indices: 3- most sensitive; 2- moderately sensitive; 1- least sensitive; and 0-when not sensitive at all.

From the sensitivity matrix shown in Table 2, it is evident that all three-sensor signals show a varying degree of sensitivity to changes in the process parameter in all three directions. The y- and z-dynamic forces, x- and z-static forces, and x- and z-acceleration were the most sensitive as their sum total response were largest. Bearing in mind that a score of 9 was the highest absolute total response, any score

above 5 would be indicative of good sensitivity to changes in the cutting conditions. Inspection of the matrix indices table shows that 6 components scored 5 and above. Effectively, the y-, x- and y-components of the static forces, STP dynamic forces and acceleration signals respectively were less sensitive to process parameter changes.

FREQUENCY SPECTRA ANALYSES

The interpretation of the frequency analysis results was carried out through spectra displays and contour plots. Each plot was presented as a series of three displays:

The complete frequency spectrum (15 kHz)

With a cut-off frequency at 5 kHz, and

With a cut-off frequency at 2 kHz.

To aid clarification, the cutting conditions have been omitted in the graphs but the following table gives the variable designations used.

Inspection of the obtained spectra and contour plots showed that there was a consistent peak at 500 Hz, 2-4 kHz, and 8-10 kHz. With the vibration spectra, the higher frequency components were dominant whereas the 2-4 kHz components were sharpest on the dynamic force spectra. The lower frequency band was rather difficult to interpret. This frequency was most likely to be associated with chip breaking and the approximate calculations of the chip fracture frequency indicated this to be the case. Change in amplitude of the chip fracture frequency as the cutting speed increased suggested far more than just a mere chip fracture frequency and therefore warranted further investigation. The effect of spindle motor speed on the frequency spectra with the lathe idle was studied. Obtained spectra results indicated that the 0-500 Hz frequency band was sensitive to spindle speed increments, and its magnitude increased proportionally to the spindle motor speed. This phenomenon was associated with background noise from the motor drive belt, linkages and the hydraulic systems. The noise could not be eliminated since chip formation and fracture also had a similar frequency range. No other peaks or higher frequency bands appeared.

Effects of Cutting Speed

The cutting speed did not seem to have any substantial effects on the magnitude of the dynamic and vibration signals in the spectra (Figs. 14-16). As expected, an increase in the magnitude of the peak at 500 Hz was visible when increasing cutting speed for reasons already outlined. Unlike the dynamic force spectra with no apparently noticeable features, the acceleration spectra peaks shifted from 2-3 kHz band to concentrate in the 10 kHz band (i.e. increasing the cutting speed altered the chip lamination frequency).

Feed Rate

The general effect on the dynamic force spectra (Figs. 17 & 18) was an increase in the bandwidth of the resonant frequencies at 2-4 kHz and 10 kHz. These observations were visible on the three force components, with visualisation being stronger on the z-component, and weakest on the x-components. Inspection of the vibration spectra showed that the 10 kHz peak was the most sensitive to feed rate

changes. Generally, peaks appeared at ≈ 5 kHz and 10-12 kHz, which tended to increase proportionally to the feed rate. However, magnitudes of the latter frequency band were more than 5 times larger than those in the former frequency band with the x-direction spectra more sensitive to feed rate changes and y-axis the least.

Effects of DOC

The 500 Hz and 2-3 kHz peak were more sensitive to DOC changes on the x- and y-dynamic force spectra. They generally increased while the 10 kHz peak remained constant and therefore less sensitive. On the z-force displays the spectra behaviour (Fig. 19) was similar to those of the x- and y-displays with the 10 kHz peak more sensitive to DOC changes. The vibration spectra (Fig 20) showed that the sharpest response occurred with the 10 kHz peak. The x-component increased as the DOC increased. This increase was also observed with the z-component but was less prominent in the y-component.

On the whole, as the DOC increased, the noise in the data tended to increase and the region of maximum concentration of the spectra energy became rather dispersed. This effect was most prominent in the z-component at a DOC of 3 mm.

Frequency analysis was undertaken mainly to identify specific directions or points that had a high dynamic tendency that could not be visualised in the time domain. The data was first passed through a forward Fast Fourier Transform (FFT) to yield the frequency distribution data, and then the FFT data was smoothed using a seventh order filter. The final data was presented as spectra and contour plots. Frequency spectra presentation allows visualisation of the sensor signal behaviour of single axis spectrum for each cutting condition. This allows a comprehensive establishment of the relationship between frequency and amplitude of the sensor signals for the complete sampled frequency range (Figs. 21-24). Contour plots show the behaviour of the complete cutting condition range (desired variable) with the complete or cut-off frequency range, thereby allowing visualisation of the dominant frequencies. Generally vertical rows of peaks on the contour plots (Figs. 25 - 29) are indicative of a resonant or dominant frequency and the more compact and close the line the steeper the peaks.

DISCUSSION

An important observation made from these tests was that under fixed sets of cutting conditions, the characteristic resonant frequencies of the tool holder and chip lamination remained constant and therefore variations on its peak frequency or bandwidth indicated sensitivity to changing parameters. It was also noticed that there was an amplitude peak at a low frequency spectrum on the free running lathe, indicative of substantial noise from the electric motors.

This investigation demonstrates that the well-known effect of cutting speed on plane-faced tool static force behaviour was only partly valid. The first discrepancy involved the cutting forces remaining largely unchanged as the cutting speed increased. Normally, slight reductions in the force components accompany moderate to high cutting speed increases for a nominally sharp plane-faced tool. The reason for this

did not seem immediately apparent, but a possible logical reason could be the tool insert geometry effect. The workpiece used in this investigation, EN24, had been hot rolled, quenched in oil and tempered, and was considerably hard to machine. The normal or expected trend, based on studies where machining was performed using plane-faced tool inserts and the only variable being the cutting speed, would have been a slight decrease in the static cutting force components with an increase in cutting speed. Most of the obtained plots showed that the static cutting forces tended to remain constant with very slight variation as the surface cutting speed increased. It could be argued that the relative hardness of the workpiece was the main contributing factor. With the slight decrease in static cutting forces due to increases in the cutting speed offset by wear effects.

Another significant contribution to the uniqueness of this study is the supposed effect of mechanical and chemical interaction between the tool insert and the workpiece. Unlike the results obtained in Dimla [6], which involved the use of uncoated inserts, the wear mechanisms were deemed to have been significantly altered by the current coated tool inserts. Possible reasons for the high wear resistance of these inserts were the reduction in abrasion and diffusion wear (especially abrasion wear) in the primary and secondary phases of tool wear. Naturally, if two materials of equal hardness are rubbed together, it takes a long time and considerable effort to scratch their surfaces i.e. harder materials have high abrasion resistance. Beyond the secondary phase i.e. on the threshold of the tertiary phase, the wear rate was found to accelerate as the abrasion resistance was weakened, resulting in the erosion of the coating, and plastic deformation of the cutting edges. This phenomenon was primarily due to changes in the coating thickness, thermal reduction of the cohesive strength of the materials, an increase in the coefficient of friction between coating layer and chips, and elastic properties of the substrate deposit [9].

The similarity between the current results and those from plane-faced tool insert geometry with respect to static force components were expected, i.e. a larger magnitude for the main cutting force (F_z), similar radial cutting force (F_x) and a smaller axial force (F_y).

Chip formation depended largely on the cutting conditions. Both types of chip patterns, continuous and discontinuous, were simultaneously produced. The discontinuous chip formation in these experiments was a direct consequence of the utilisation of chip-breaker geometry tool insert, i.e. controlled tool chip contact. This was partly due to the danger that uncontrolled chip formation posed to the machine operator, and to a lesser extent, chipping of the cutting tool edge by any entangled chip. Another consideration in utilising chip breaker configuration was to reduce the volume of solid chip material. While unbroken continuous chip has a bulk ratio of ≈ 50 , broken chips have a bulk ratio of ≤ 3 , offering a volumetric reduction of more than 17 times, serving handling and removal time, and cost [10]. The use of the chip breaker configuration inserts in this study was first and foremost to control and break the chip (i.e. integral obstruction).

CONCLUSIONS

Based on the results discussed herein, the effects of the cutting parameters on the sensor signals cannot be ignored. All three cutting conditions affect the magnitude of the process parameters (feed rate and DOC) or the rate of tool wear (cutting speed). In order to develop what might be termed a universal tool condition monitoring system, it is prudent not to limit the operational functioning range of the system, hence the reason for using all three cutting parameters as independent inputs to the envisaged system.

Feed rate and DOC principally influenced increases in the force components with other changes attributable to a combination of factors such as tool wear and material non-homogeneities.

REFERENCES

- [1] Shaw, M. C. (1984), 'Metal Cutting Principles', Clarendon Press, Oxford Chapter 3, pp 18-46.
- [2] Boothroyd, G. (1975), 'Fundamental of metal machining and machine tools', 1st Ed. Scrupta Book Company.
- [3] Kalpakjian, S. (1991), 'Manufacturing Processes for Engineering Materials', 2nd Edition, Chapter 8, pp 473-581, Addison-Wesley Publication Company.
- [4] Trent, E. M. (1977), 'Metal Cutting', Butterworths.
- [5] Radford, J. D. and Richardson, D. B. (1974), 'Production Engineering Technology', the MacMillan Press Ltd., London, Chapter 7, pp 119-155.
- [6] Dimla, D. E. (2004) The Impact of Cutting Conditions on Cutting Forces and Vibration Signals during Turning with Plane Face Geometry Inserts. J. Mat. Processing Tech. 155-156, 1708-1715.
- [7] Dimla, D. E. and Lister, P. M. (2000a) On-line metal cutting tool condition monitoring - Part I: Force and Vibration analyses. Int. J. Machine Tools & Manufacture, Vol. 40 No. 5, pp. 736-768.
- [8] Dimla, D. E. and Lister, P. M. (2000b) On-line metal cutting tool condition monitoring - Part II: Multi-layer perceptron neural networks analysis. Int. J. Machine Tools & Manufacture, Vol. 40 No. 5, pp. 769-781.
- [9] Dimla, D. E. (1998) Multivariate tool condition monitoring in a metal cutting operation using ANNs. PhD Thesis, School of Engineering, University of Wolverhampton, UK.
- [10] Sandvik Coromant, AB (1995) Metal Working Products Catalogue-Turning Tools
- [11] D. Guinea, A. Ruiz and L. J. Barrios (1991) Multi-sensor integration- An automatic feature selection and state identification methodology for tool wear estimation. Computers in Industry, Vol. 17. pp 121-130.

APPENDIX

A1. Signal Processing

The noisy nature of the captured sensor signals required an active selection or mapping of features from the sampled sensor signals. Features were selected by a heuristic trial and error approach, based on certain physical considerations, e.g. mean as representative of the time variation and first order frequency transformation [11].

The signal-processing paradigm consisted of five distinct stages. In the first stage, the data was uploaded into MATLAB environment memory and the static force components of the cutting force calculated as the mean of the complete sampled cutting force signal. In the second stage, the dynamic force was calculated by using the previously obtained mean by subtracting the mean value of force from each sampled data point. The next stage was to obtain the Fast Forward Transform (FFT) of the dynamic signals (dynamic force and vibration). The dynamic force data was first windowed through application of a Hanning window before its FFT calculated for repeatability of the record length throughout. The obtained FFT data was then smoothed using a seventh order factor to enhance the quality of any visual plots (spectra and contour plots).

A2. Algorithm Description

1. The data whose FFT was required was multiplied by $\cos^2(t)$ - the Hanning window function which is essentially a bell-shaped function spanning $-\pi/2$ to $\pi/2$ in order to reduce signal leakage that otherwise would mask small frequencies.
2. The FFT of each data point was calculated and its negative component was taken into account by considering the RMS value corresponding to each frequency, and this was calculated and normalised (dividing by N). i.e.

$$P_{RMS}(f_k) = \frac{1}{N} \sqrt{2 R_k^2} \quad (i)$$

where f is the sampling frequency, k is the i^{th} variable number of sample, N is the total number of samples, P is the power RMS value, and R is the resolution of signal.

3. Since only the power or energy distribution in certain frequency band was of interest, it was not necessary to obtain the complete energy distribution in the entire frequency range. Therefore, the total power in the FFT spectrum from $f_k = 0$ to $f_k = N/2$ was considered i.e.

$$P_{Total}(f_{\frac{N}{2}}) = \sum_{k=1}^{\frac{N}{2}+1} \frac{1}{N} \sqrt{2 R_k^2} \quad (ii)$$

The $k=0$ value corresponded to the dynamic force DC value in the FFT range, and since it was not affected by the transformation, it was neglected.

When spectra plots were required for visual confirmation of features, a smoothing filter was used to enhance and smooth the curve. This simply replaced the concerned point with its mean i.e. for a 7th order filter, the smoothing began at the 4th data point, replacing it with the mean of the first three ahead and the three previous data points.

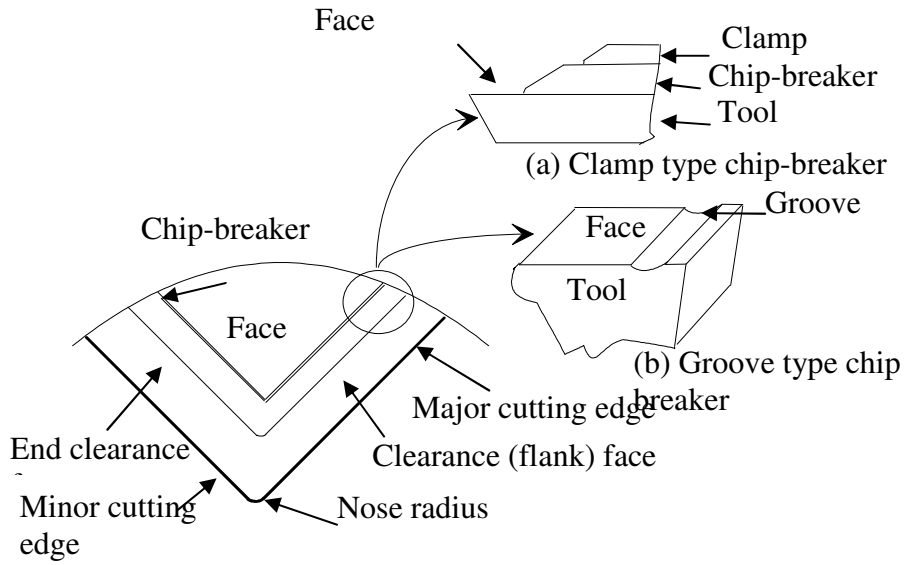


Fig. 1. Cutting tool terminology.

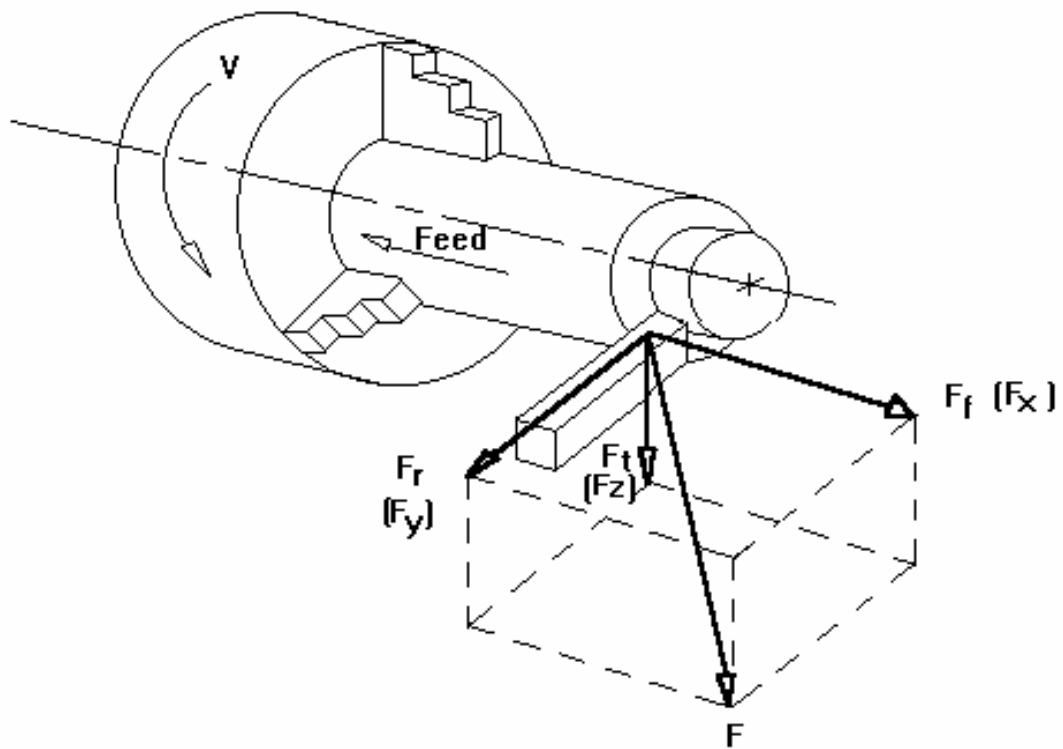


Fig. 2. Forces acting on a cutting tool in orthogonal metal cutting.

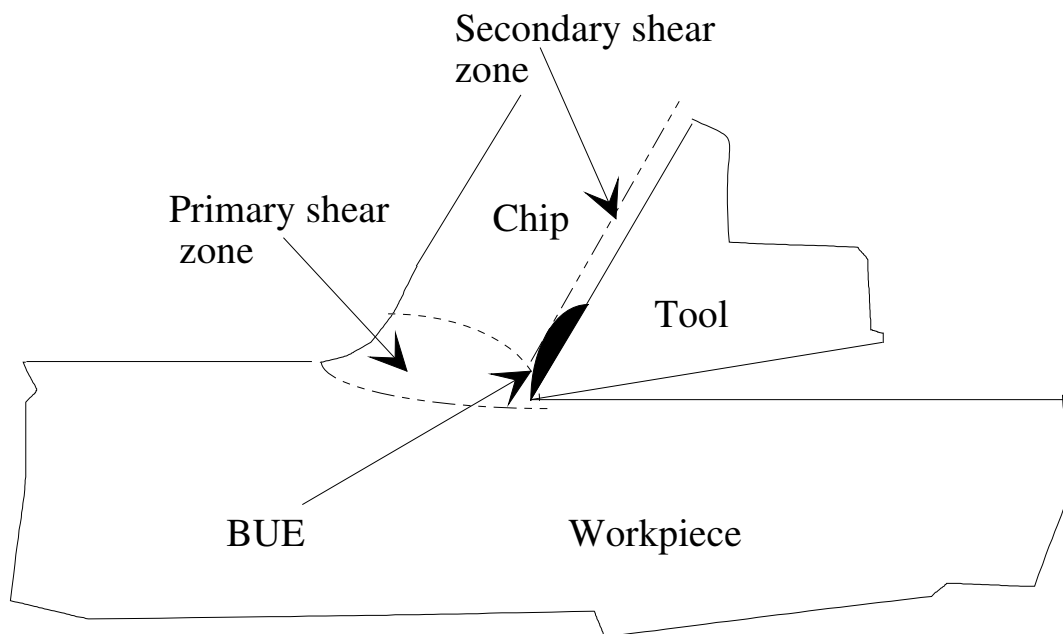


Fig. 3. Metal cutting shear zones and BUE.

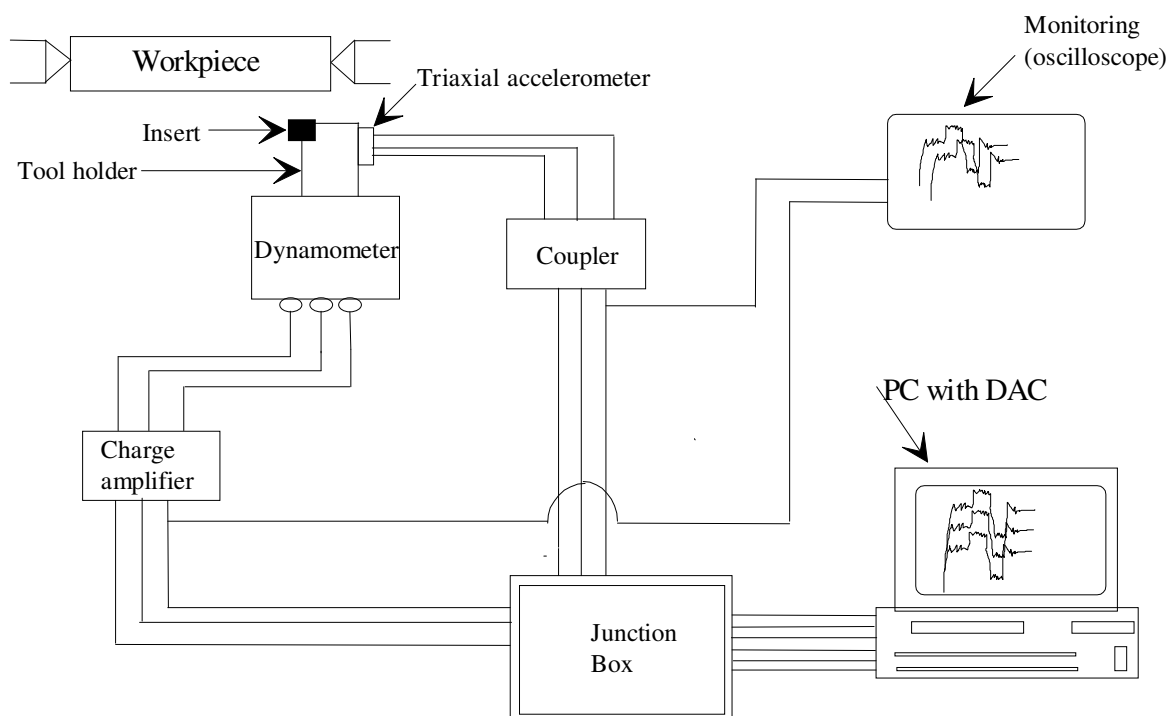


Fig. 4. Schematic diagram of the experimental test rig.

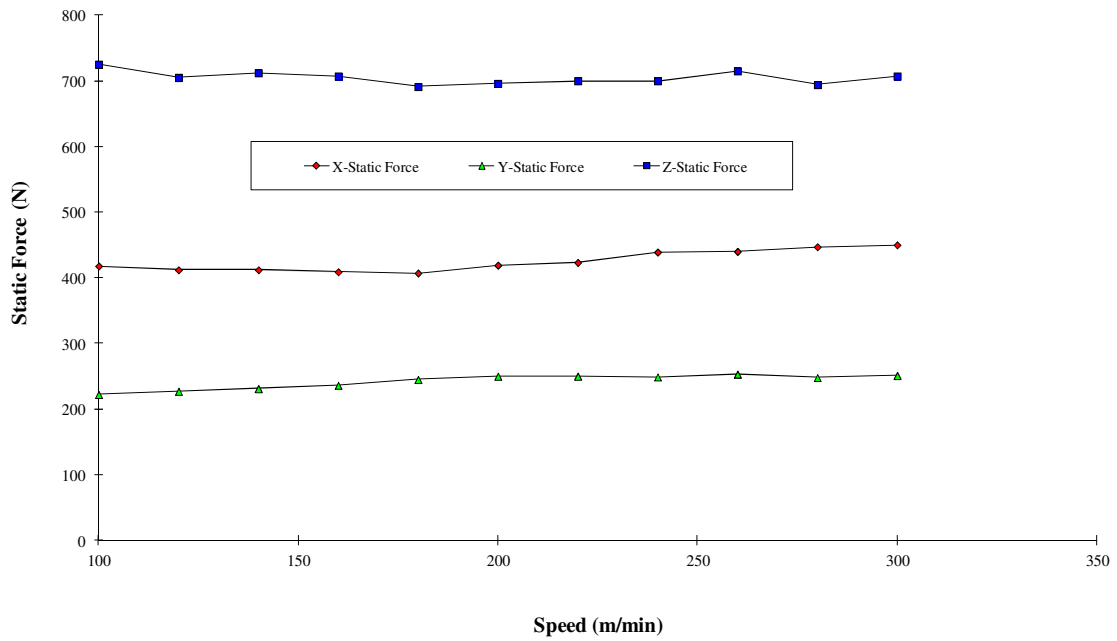


Fig 5. Static force - cutting speed ($f=0.2\text{mm/rev.}$ & $a=2\text{mm}$).

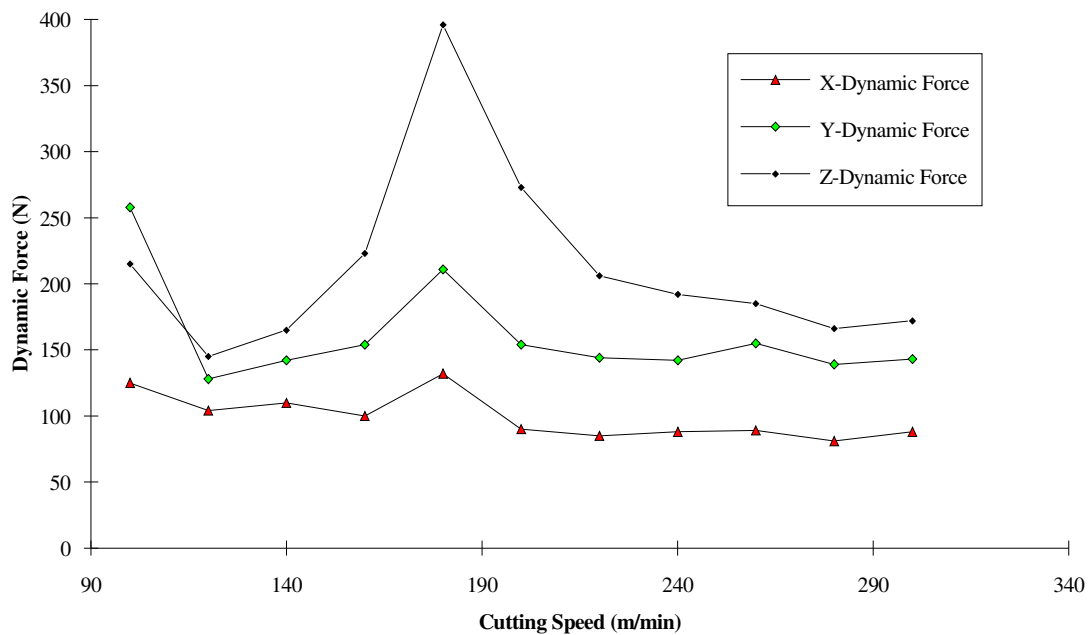


Fig 6. STP dynamic force - cutting speed ($f=0.2\text{mm/rev.}$ & $a=2\text{mm}$).

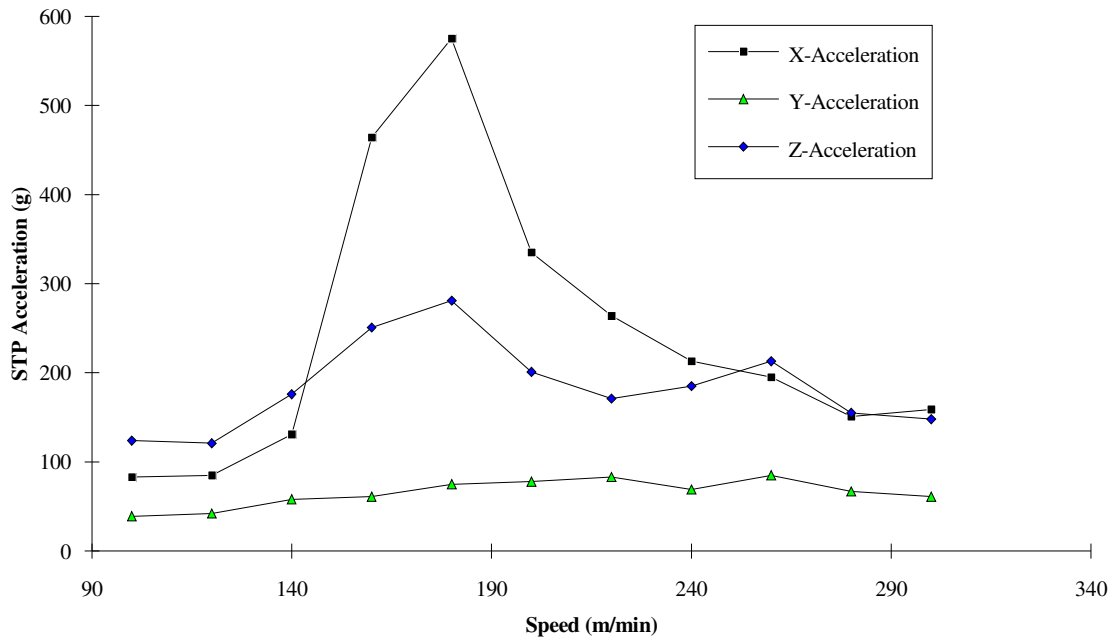


Fig 7. STP acceleration - cutting speed (f=0.2mm/rev. & a=2mm).

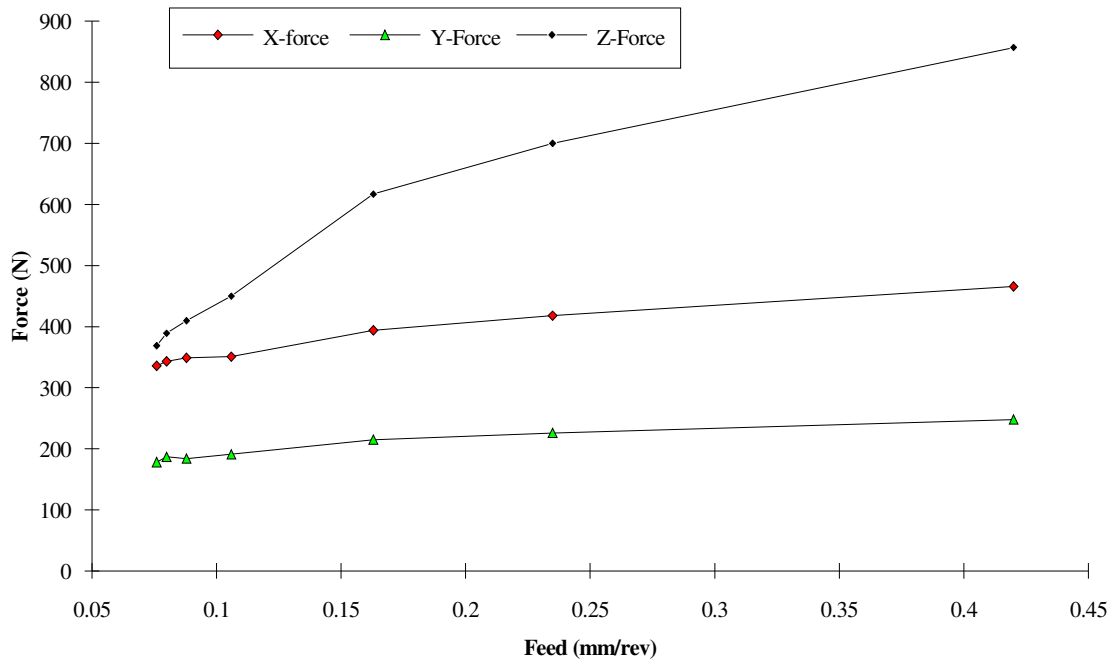


Fig 8. Static force - feed rate (V=200m/min. & a=2mm).

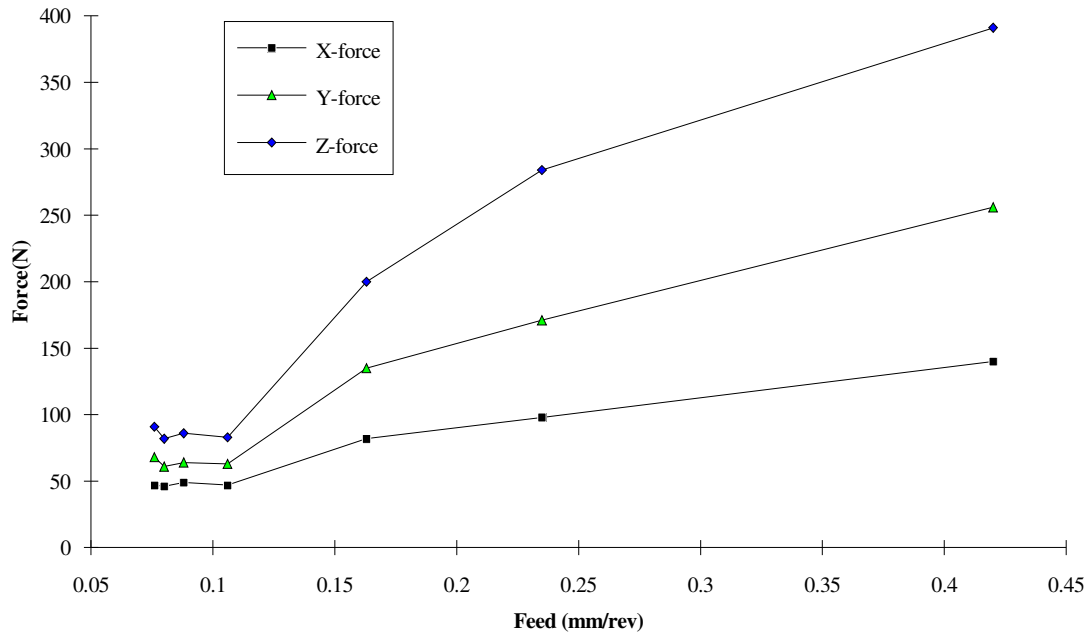


Fig 9. STP dynamic force - feed rate (V=200m/min. & a=2mm).

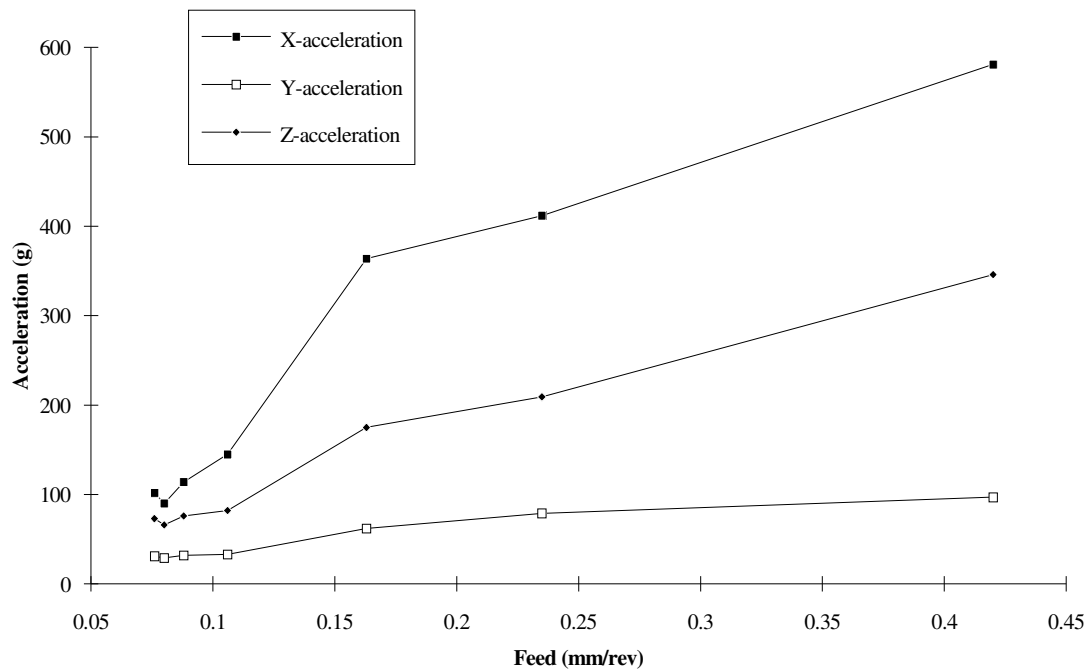


Fig 10. STP acceleration - feed rate (V=200m/min. & a=2mm).

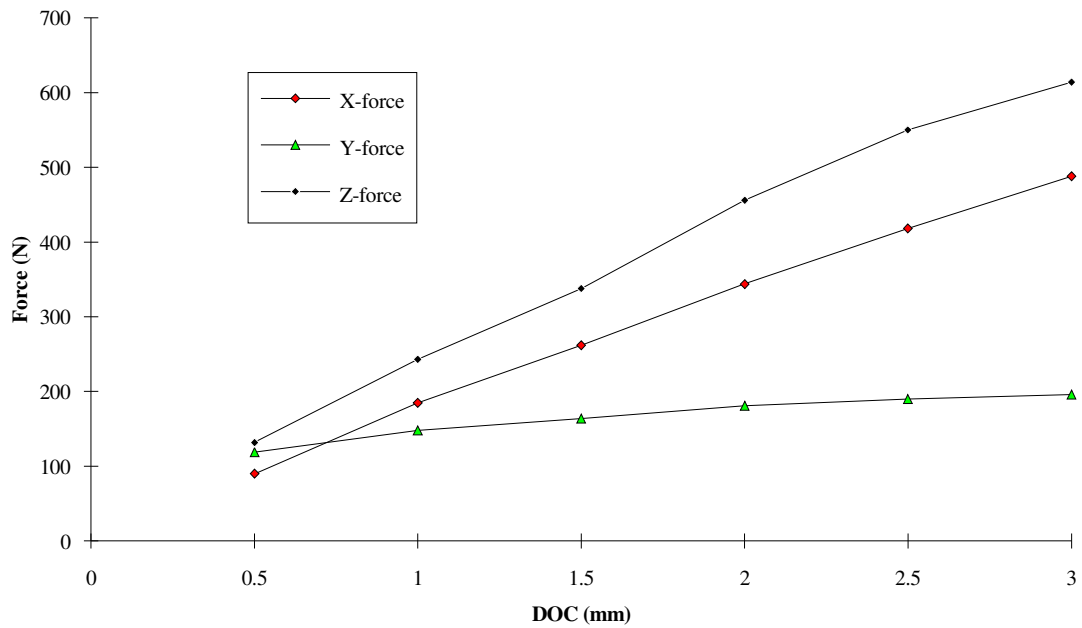


Fig 11. Static force – DOC (V=200m/min. & f=0.2mm/rev.).

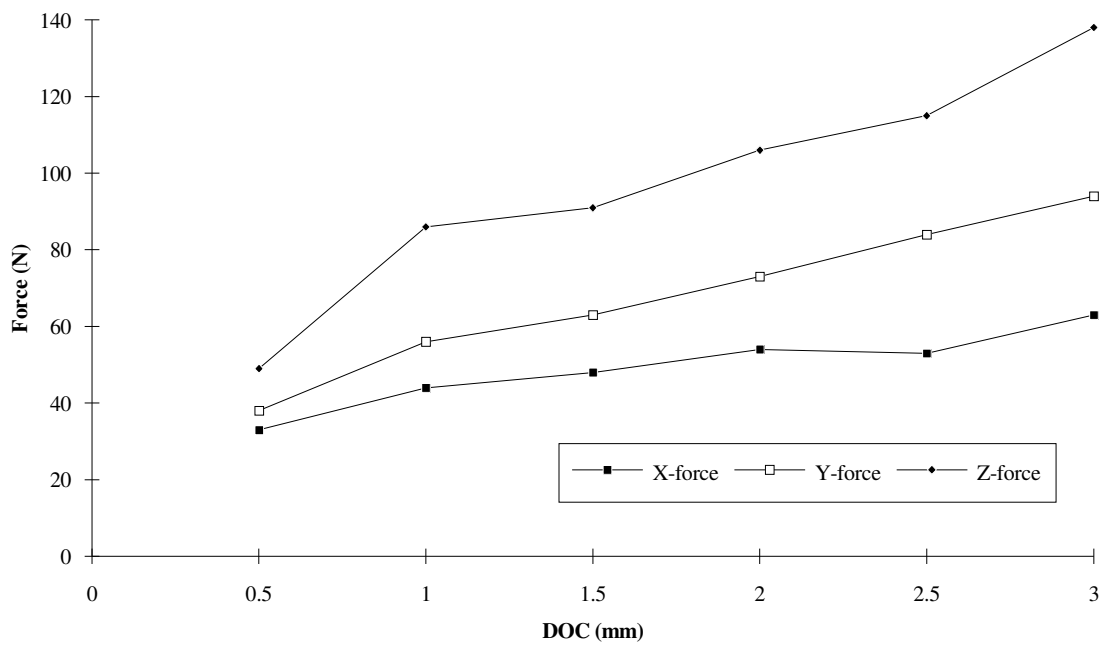


Fig 12. STP dynamic force - DOC (V=200m/min. & f=0.2mm).

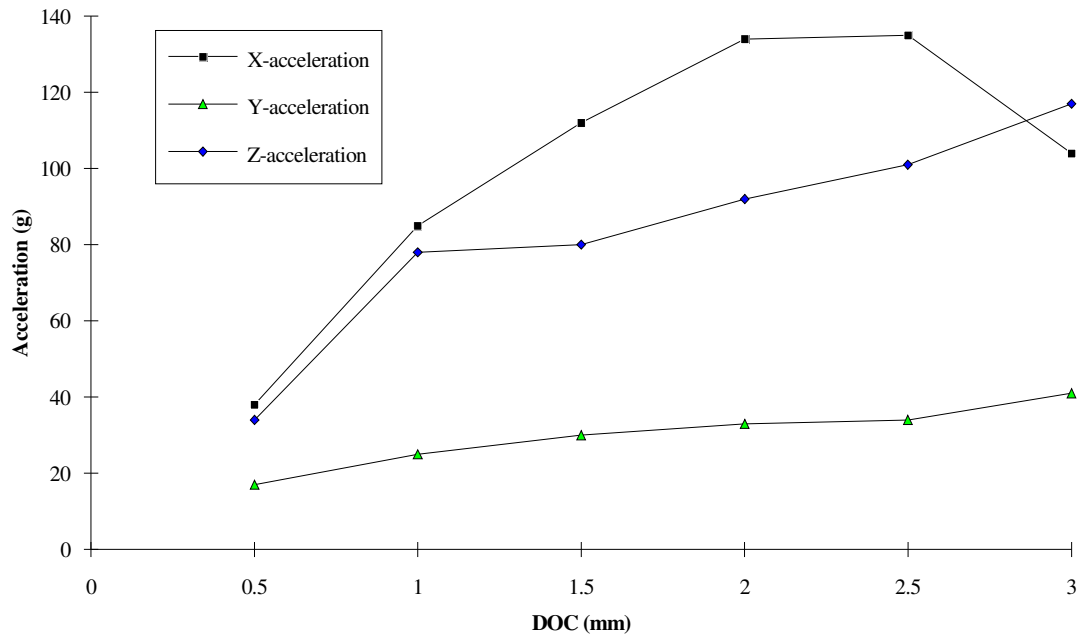


Fig 13. STP acceleration - DOC ($V=200\text{m/min.}$ & $f=0.2\text{mm/rev.}$).

Y-Dynamic Force Spectra

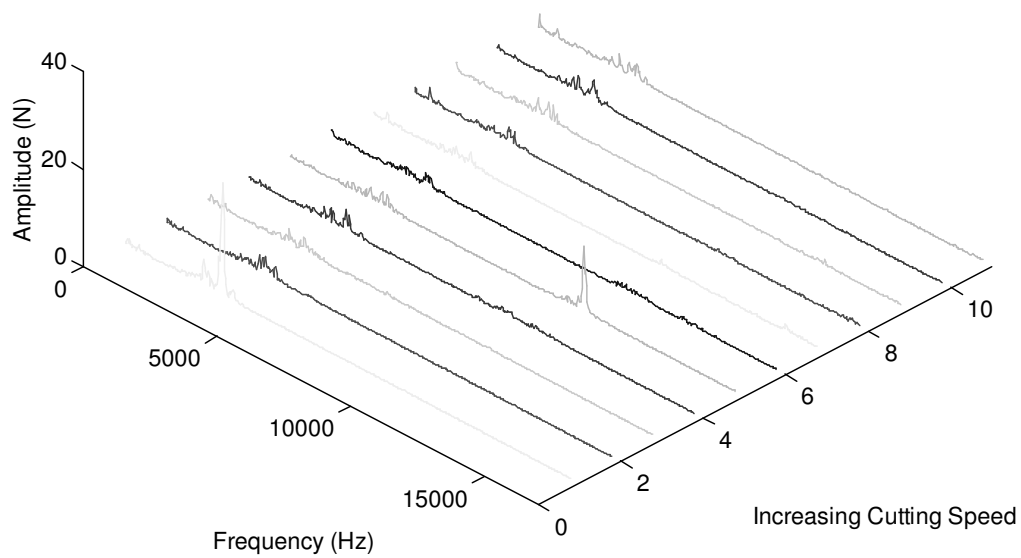


Fig 14. Y-dynamic force spectra - cutting speed ($f=0.2\text{mm/rev.}$ & $a=2\text{mm}$).

X-Vibration Spectra

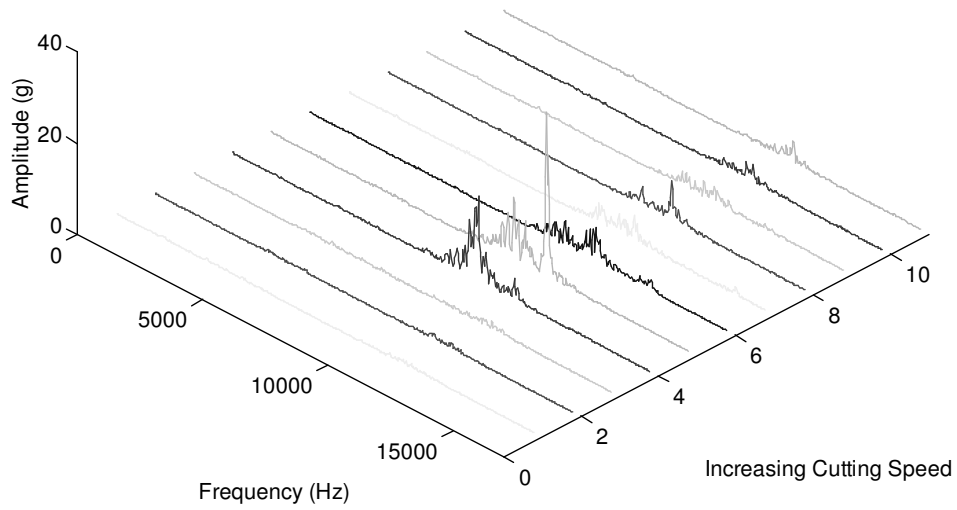


Fig 15. X-vibration spectra - cutting speed ($f=0.2\text{mm/rev.}$ & $a=2\text{mm}$).

Y-Vibration Spectra

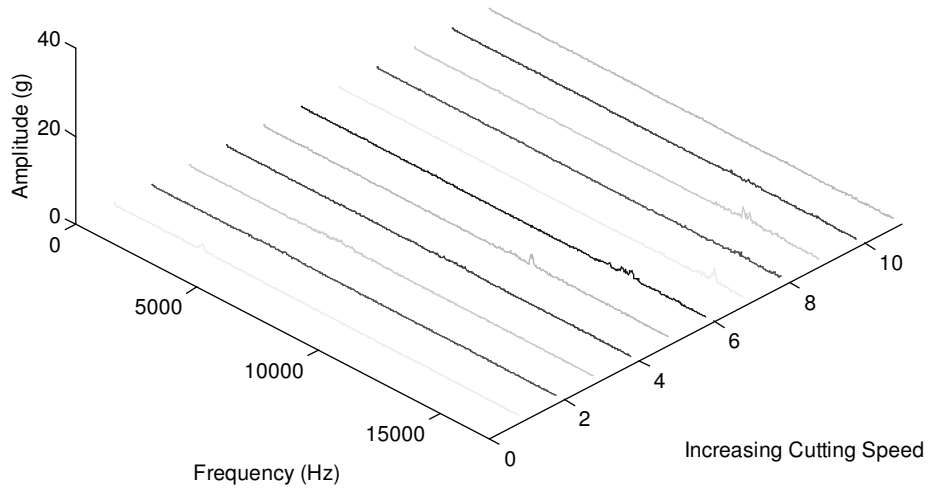


Fig 16. Y-vibration spectra - cutting speed ($f=0.2\text{mm/rev.}$ & $a=2\text{mm}$).

Z-Dynamic Force Spectra

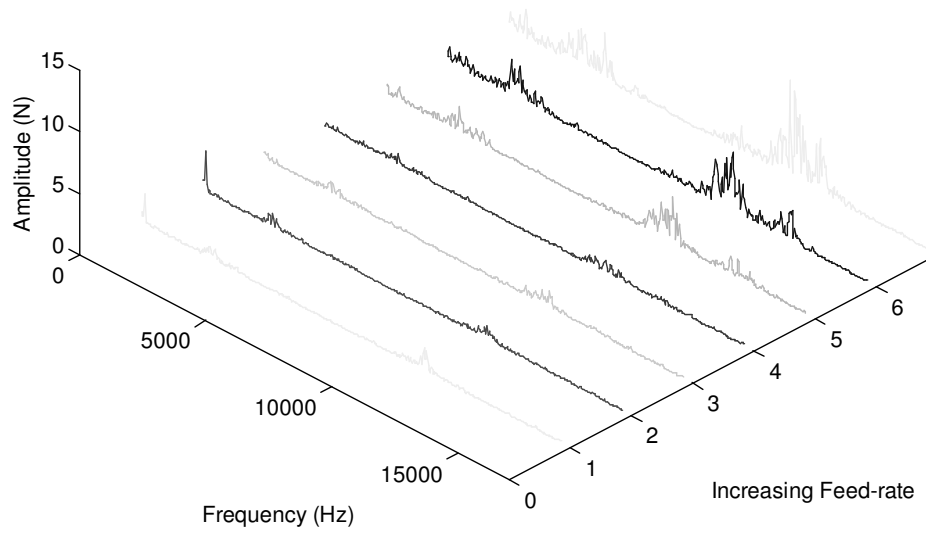


Fig 17. Z-dynamic force spectra - feed rate ($V=200\text{m/min.}$ & $a=2\text{mm}$).

Z-Vibration Spectra

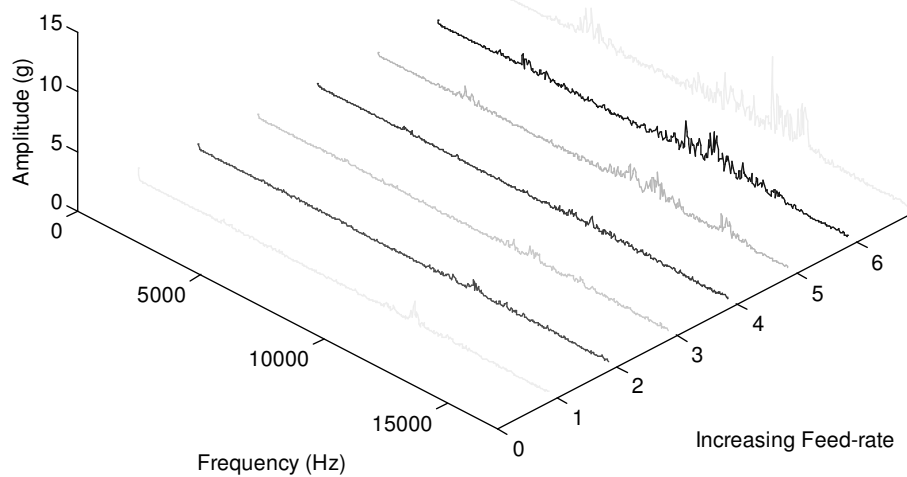


Fig 18. Z-vibration spectra - feed rate ($V=200\text{m/min.}$ & $a=2\text{mm}$).

Z-Dynamic Force Spectra

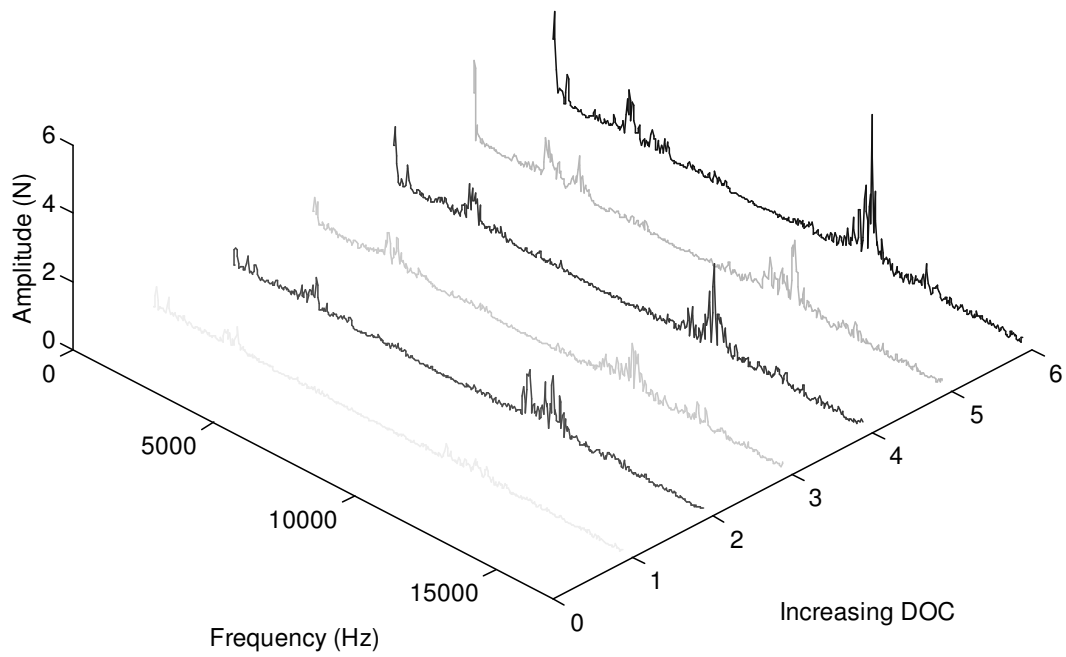


Fig 19. Z-dynamic force spectra - DOC (V=200m/min. & f=0.2mm).

X-Acceleration Spectra

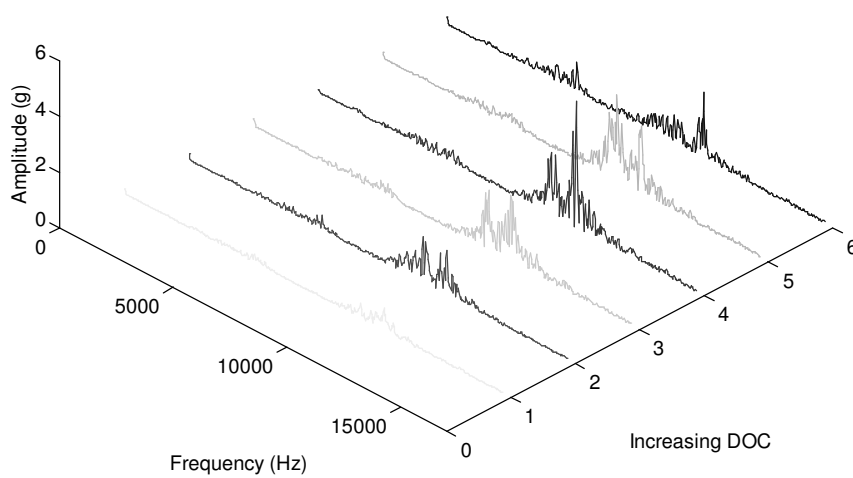


Fig. 20. X-vibration spectra - DOC (V=200m/min. & f=0.2mm/rev.).

Z-Dynamic Force Spectra

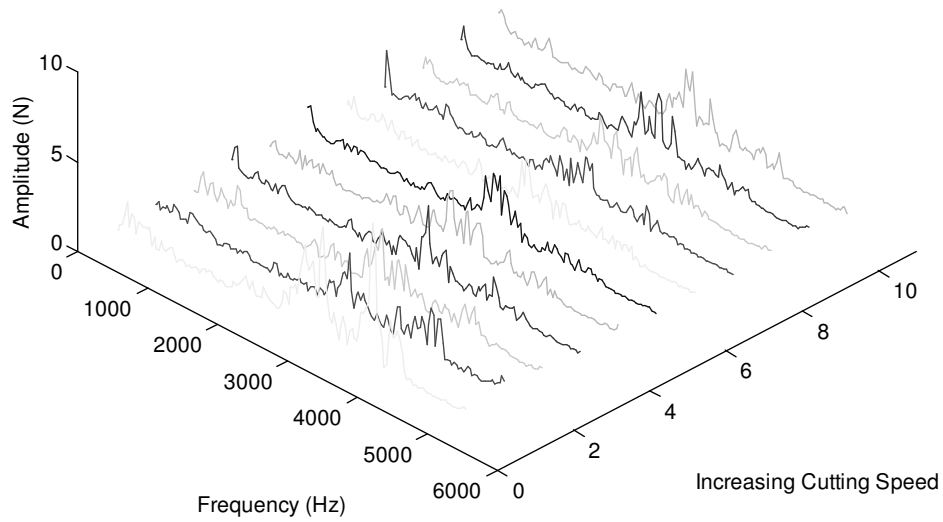


Fig. 21. Z-dynamic force spectra - cutting speed - 5 KHz cut-off ($f=0.2\text{mm/rev.}$ & $a=2\text{mm}$).

Z-Vibration Spectra

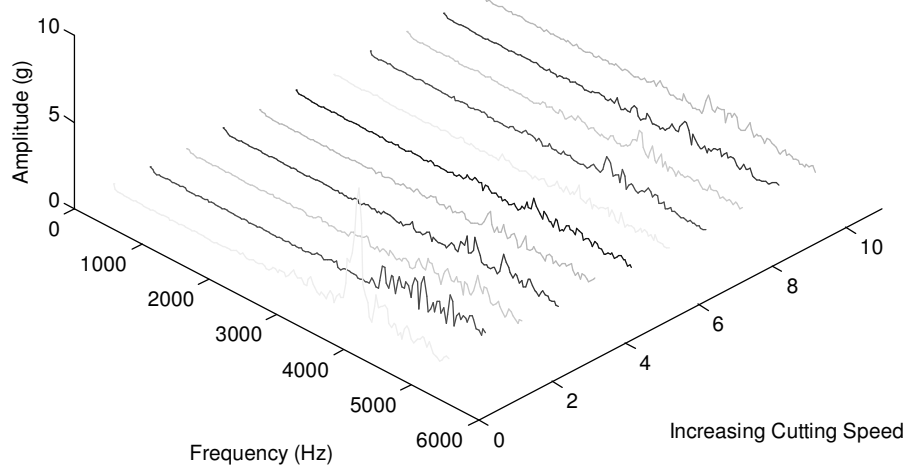


Fig 22. Z-vibration spectra - cutting speed - 5KHz cut-off ($f=0.2\text{mm/rev.}$ & $a=2\text{mm}$).

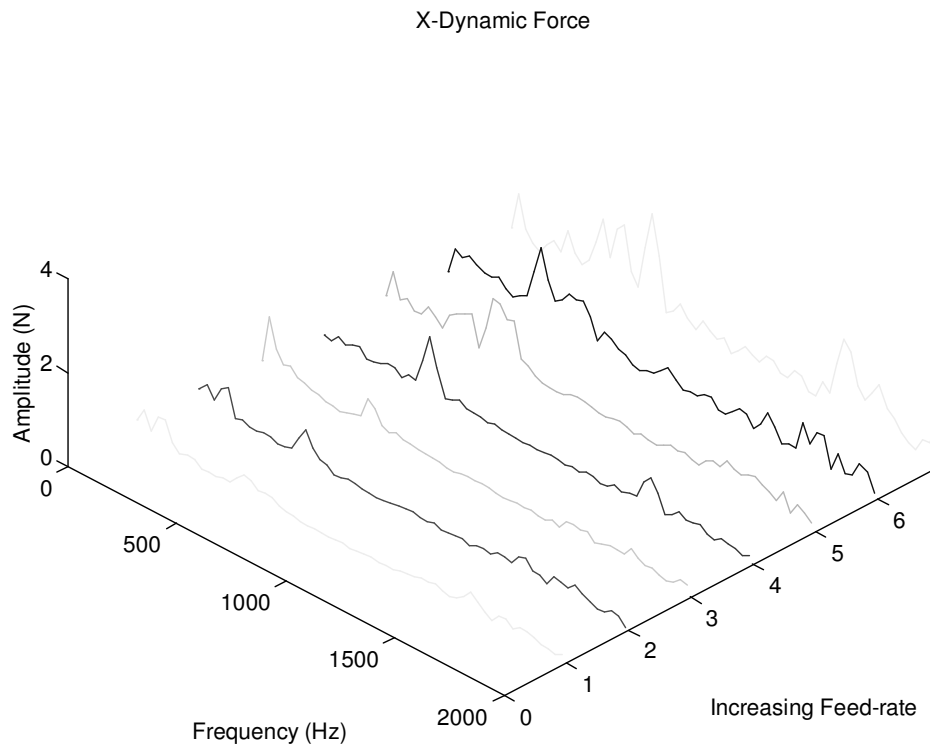


Fig. 23. X-dynamic force spectra - feed rate - 2 KHz cut-off ($V=200\text{m/min.}$ & $a=2\text{mm}$).

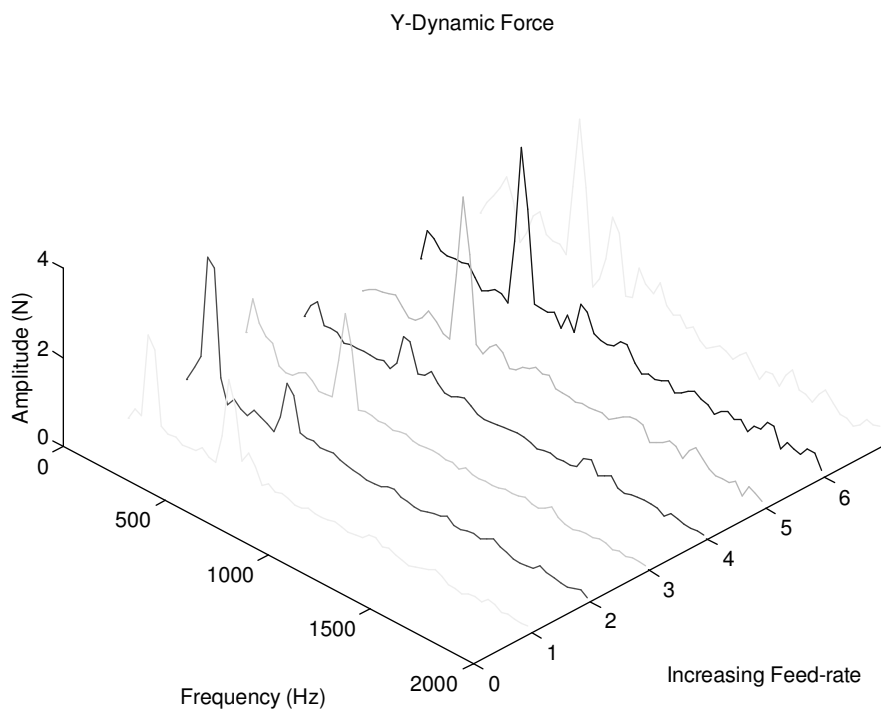


Fig. 24. Y-dynamic force spectra - feed rate - 2 KHz cut-off ($V=200\text{m/min.}$ & $a=2\text{mm}$).

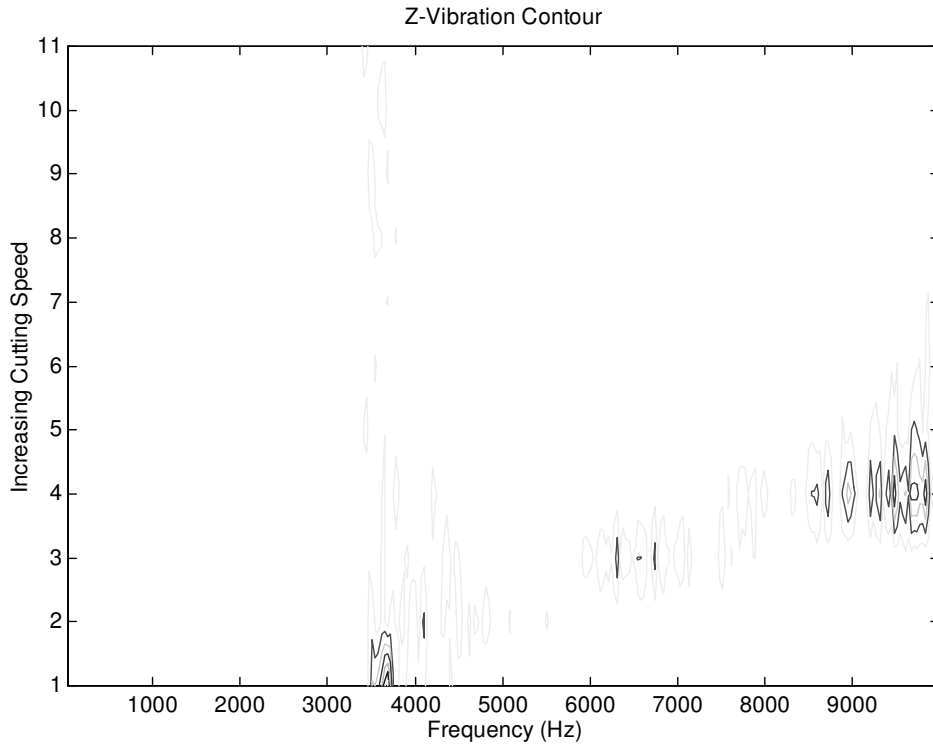


Fig. 25. Z-vibration contour - cutting speed ($f=0.2\text{mm/rev.}$ & $a=2\text{mm}$).

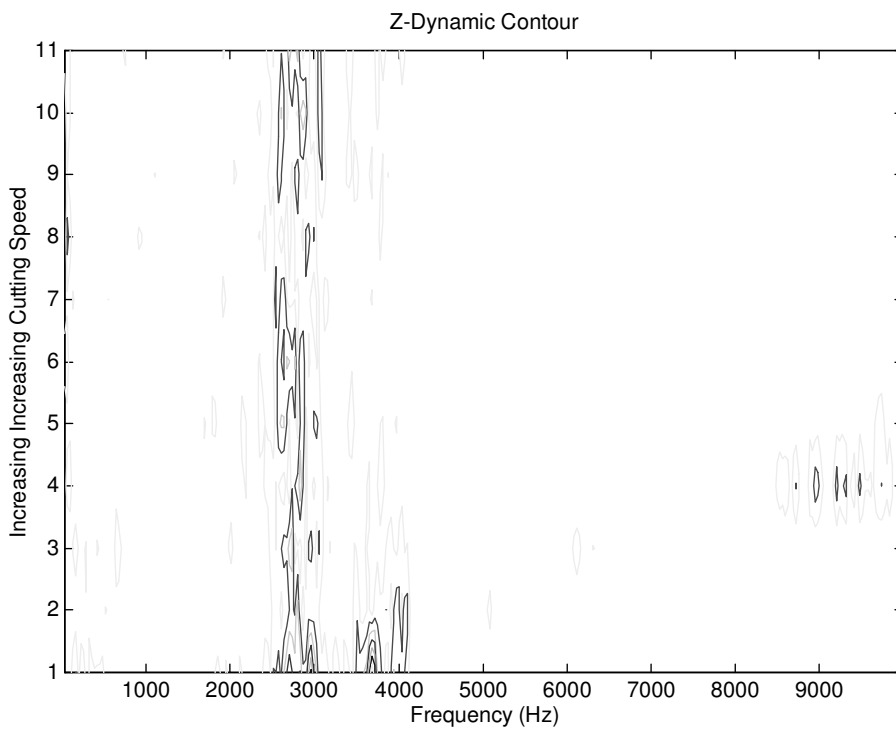


Fig 26. Z-vibration contour - cutting speed ($f=0.2\text{mm/rev.}$ & $a=2\text{mm}$).

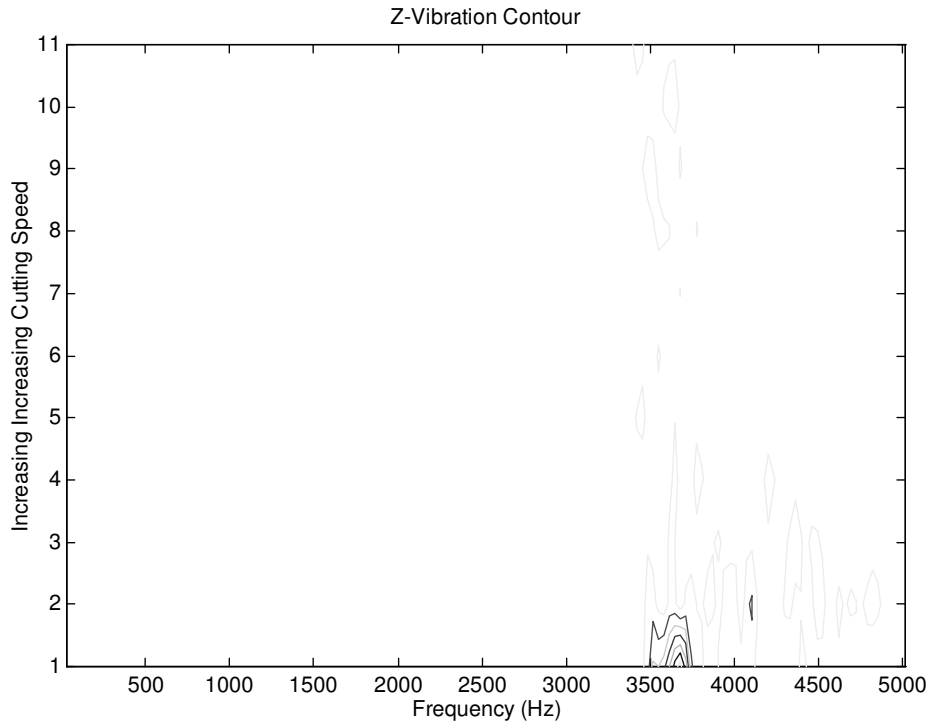


Fig. 27. Z-vibration contour - cutting speed (cut-off at 5 KHz) ($f=0.2\text{mm/rev.}$ & $a=2\text{mm}$).

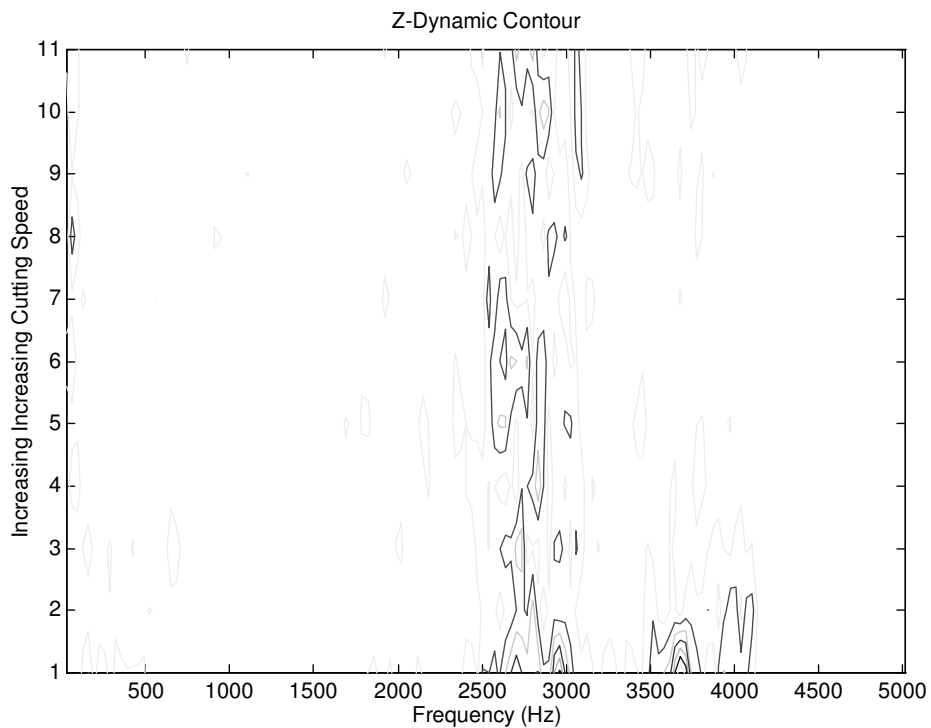


Fig. 28. Z-vibration contour - feed rate (cut-off at 5 KHz) ($V=200\text{m/min.}$ & $a=2\text{mm}$).

Table 1: Details of cutting material and cutting conditions.

Machine Tool		Lang J6
Workpiece Material		
	Work Material	EN24T BS 970 817M40
	Hardness	Brinell 255
	Composition	0.4% C, 0.28% Si, 0.27% Mo 1.18% Cr, 0.5 % Mn, 1.4% Ni
Tooling Material:	Tool Holder	Sandvik SSBCR 2020 K12
	Tool Type	SCMT 12 04 08 UM
	Tool Material	Sandvik Coromant P15 4015
	Overhang (mm)	50
Cutting Conditions	Speed (m/min.)	100 - 300 @ 20 intervals
	Feed (mm/rev)	0.08 - 0.42 (5 values between)
	Depth /mm	0.5 - 3 @ 0.5 intervals
Cutting fluid	None	

Table 2: Sensitivity matrix index.

Process Parameter	Static Force			Dynamic Force			Vibration		
	x	y	z	x	y	z	x	y	z
Speed	1	1	1	1	2	3	3	1	2
Feed	2	1	3	1	2	3	3	1	2
DOC	2	1	3	2	2	3	3	1	3
Total Response	5	3	7	4	6	9	9	3	7

Table 3: Key to waterfall and contour plots.

Variable Designation	Cutting Speed (m/min)	Feed rate (m/rev)	DOC (mm)
1	100	0.076	0.5
2	120	0.08	1
3	140	0.09	1.5
4	160	0.1	2
5	180	0.16	2.5
6	200	0.24	3
7	220	0.42	
8	240		
9	260		
10	280		
11	300		